A new potential anti-cancer beta-carboline derivative decreases the expression levels of key proteins involved in glioma aggressiveness: a proteomic investigation

Running title: Proteomics of CM16 β-carboline against gliomas

Annelise Carvalho, PhD[a,b], Johan Viaene, PhD[c], Guy Vandenbussche, PhD[d], Kris De Braekeleer, PhD[e], Bernard Masereel, PhD[f], Johan Wouters, PhD[f], Florence Souard, PhD[e,g], Yvan Vander Heyden, PhD[c], Pierre Van Antwerpen, PhD[e,h], Cédric Delporte, PhD[e, h*], Véronique Mathieu, PhD[a,b*]

[a]Department of Pharmacotherapy and Pharmaceutics, Faculté de Pharmacie, Université Libre de Bruxelles, Brussels, Belgium
[b]ULB Cancer Research Center, Université Libre de Bruxelles, Brussels, Belgium
[c] VUB –Analytical Chemistry, Applied Chemometrics and Molecular Modeling, Pharmaceutical Institute, Vrije Universiteit Brussel – VUB, Brussels, Belgium
[d] Laboratory for the Structure and Function of Biological Membranes, Faculté des Sciences, Université Libre de Bruxelles, Brussels, Belgium
[e] Unity of Pharmacognosy, Bioanalysis and Drug Discovery, Department of Research in Drug Development (RD3), Faculté de Pharmacie, Université Libre de Bruxelles, Brussels, Belgium
[f] NAMEDIC, Department of Pharmacy, University of Namur, Namur, Belgium
[g]Univ. Grenoble Alpes, CNRS, DPM, 38000 Grenoble, France
[h] Analytical Platform of the Faculty of Pharmacy and Laboratory of Pharmaceutical Chemistry, Faculty of Pharmacy, Université Libre de Bruxelles, , Brussels, Belgium.

[*]**Correspondence to:**

Véronique Mathieu, MD, PhD
Department of Pharmacotherapy and Pharmaceutics – Faculté de Pharmacie – Université Libre de Bruxelles [ULB], biology
Campus de la Plaine – Boulevard du Triomphe – 1050 Brussels – Belgium.
Tel: +32 478 317 388
E-mail: vemathie@ulb.ac.be

Cédric Delporte, PhD
Unity of Pharmacognosy, Bioanalysis and Drug Discovery, Department of Research in Drug Development (RD3), and Analytical Platform of the Faculty of Pharmacy and Laboratory of Pharmaceutical Chemistry, Faculty of Pharmacy, Université Libre de Bruxelles [ULB], LC MS and auto MS/MS
Campus de la Plaine – Boulevard du Triomphe – 1050 Brussels – Belgium.
Tel: +32 2 650 52 77
E-mail: cedric.delporte@ulb.ac.be

Abstract

Gliomas remain highly fatal due to their high resistance to current therapies. Deregulation of protein synthesis contributes to cancer onset and progression and is a source of rising interest for new drugs. CM16, a harmine derivative with predicted high blood-brain barrier penetration, exerts antiproliferative effects partly through translation inhibition. We evaluated herein how CM16 alters the proteome of glioma cells. The analysis of the gel-free LC/MS and auto-MS/MS data showed that CM16 induces time- and concentration- dependent significant changes in the total ion current chromatograms. In addition we observed spontaneous clustering of the samples according to their treatment condition and their proper classification by unsupervised and supervised analyses respectively. A 2D gel-based approach analysis allowed us to identify that treatment with CM16 may downregulate four key proteins involved in glioma aggressiveness and associated with poor patient survival (HspB1, BTF3, PGAM1 and cofilin), while it may upregulate galectin-1 and Ebp1. Consistently with the protein synthesis inhibition properties of CM16, HspB1, Ebp1 and BTF3 exert known roles in protein synthesis. In conclusion, the downregulation of HspB1, BTF3, PGAM1 and cofilin bring new insights in CM16 antiproliferative effects, further supporting CM16 as an interesting protein synthesis inhibitor to combat glioma.

Key words: beta-carboline, cancer, glioma, protein synthesis, BTF3, PGAM1, HspB1

Introduction

Although primary brain tumors account for just 1.4% of all cancers, they have a high fatality rate of 60% (Strong et al., 2015). Gliomas are the most common type (~80%), accounting for the majority of the brain tumors with a poor prognosis (Ostrom et al., 2014). The poor survival rate of glioma patients has been attributed to various features, including their high invasion level (Paw, Carpenter, Watabe, Debinski, & Lo, 2015), resistance to pro-apoptotic stimuli triggered by radio- and chemotherapies, especially observed with glioma stem cells (Beier, Schulz, & Beier, 2011; Frosina, 2009), and the lack of drugs crossing the blood-brain barrier (BBB) (Azad et al., 2015).

Harmine is a natural β-carboline displaying antiproliferative and antitumor effects (Dai et al., 2012; Radhakrishnan et al., 2016; Zhang et al., 2014) through DNA intercalation and DYRK1A inhibition (Cao et al., 2005; Pozo et al., 2013; Radhakrishnan et al., 2016; Seifert, Allan, & Clarke, 2008). Despite its antitumor potential, the neurotoxicity caused by harmine *in vivo* limited its development for therapeutic uses (Cao et al., 2004; Chen et al., 2004). Thus, other harmine derivatives with different number of substituents were synthetized and tested for their antitumor potential *in vitro* and *in vivo* displaying lower toxicity than harmine and interfering with different cancer cell processes, such as cell cycle, apoptosis, angiogenesis and production of ROS (Cao et al., 2010; Guo et al., 2019; Han et al., 2012; Li et al., 2015; Luo et al., 2008; Ma, Chen, & Chen, 2016; Zhang et al., 2013; Zhang et al., 2016). In that context, the previously synthesized harmine derivative CM16 (Fig. 1a) (Meinguet et al., 2015) has been shown to display *in vitro* antiproliferative activity on various cell types including glioma models via, at least partly, an alteration of the initiation phase of protein translation (Carvalho et al., 2017).

Protein synthesis plays a pivotal role in the regulation of gene expression, especially affecting homeostasis, controlling cell proliferation, and metabolism (Hershey, Sonenberg, & Mathews,

2012). Cancer cells are characterized by a metabolic reprogramming that contributes to the different phases of tumor biogenesis including gliomas (Masuia, Caveneeb, & Mischel, 2016). In these cancers in particular, the PI3K-Akt-mTOR pathway appeared to play pivotal roles to that aim: by activating mTORC2, it contributes to Warburg effect and resistance to therapy, while it also controls protein synthesis through mTORC1 (Strickland & Stoll, 2017). Indeed, mTOR controls eIF4F assembly while MNK controls eIF4E phosphorylation (Ruggero, 2013). Additionally, the deregulated expression and activation status of translational factors has also been associated with cancer onset and progression (Hershey et al., 2012). Therefore, development of cancer cell protein synthesis inhibitory strategies is arousing growing interest in cancer research (Bhat et al., 2015). Such strategies include inhibition of specific targets in the translation machinery (Itoua Maïga et al., 2019) as well as inhibitors of upstream signaling pathways involved at different stages of cancer development (Bhat et al., 2015; Xie, Merrett, Jensen, & Proud, 2019).

Importantly, CM16, in addition to being selective to cancer cells, has been designed to meet the physicochemical properties required for drug development and is predicted to penetrate the blood-brain barrier (Meinguet et al., 2015), making this compound of potential interest against gliomas. Our previous study suggested that the inhibition of protein synthesis by CM16 might involve modification to eIF2α phosphorylation status and/or *EIF1AX, EIF3E* and *EIF3H* gene expression levels as the latter were found to be differently expressed at the mRNA level between highly and poorly sensitive cancer models among the 60 cancer cell lines panel of the National Cancer Institute (Bethesda, USA) (Carvalho et al., 2017). To gain further insights in the effects of CM16 treatment, we investigated herein the early proteomic changes triggered by CM16 in glioma cells by means of two complementary strategies i.e. a gel-free (shotgun proteomics) and a gel-based (2-D electrophoresis, 2-DE) approach using the

Hs683 human glioma cell model. We identified thereby that CM16 affects the expression levels of four proteins that play key roles in glioma progression, metabolism and migration. These potential targets could partly explain why cancer cells exhibit a higher sensitivity to CM16 than non-cancerous cell lines, even if translation *per se* has been shown to be similarly affected (Carvalho et al., 2017).

Materials and methods

Cell line and compound

The human glioma cell line Hs683 (ATCC code HTB-138) was cultivated at 37 °C and 5% CO_2 in RPMI cell culture medium (10% FBS, 200U penicillin-streptomycin, 0.1 mg/ml gentamicin and 4mM L-glutamine). The compound CM16 was synthetized as described earlier (Meinguet et al., 2015).

Protein extraction from cells and precipitation

Proteins were extracted from Hs683 cells by homogenization after addition of protease inhibitors in PBS (Roche, Brussels, Belgium). Lysates were centrifuged (100 g, 5 min) and the protein content measured by the bicinchoninic acid assay (Thermo Scientific, Leuven, Belgium). Volumes corresponding to 1mg (LC-MS shotgun) or 3mg (2-DE) were collected and proteins precipitated in 13.3% (w/v) trichloroacetic acid (Sigma Aldrich, Overijse, Belgium) in acetone containing 0.2% (w/v) dithiothreitol (Promega, Leiden, The Netherlands) according to the modified protocol from Görg et al. (Görg et al., 2000). The protein pellet was air dried and re-suspended in the appropriate solution, depending on the method of analysis (2-DE or LC-MS shotgun). For the LC-MS shotgun approach, 100 µg of ovalbumin was added to the samples as an internal standard (IS) before precipitation. Three independent experiments were carried out for the 2-DE approach and five for the LC-MS shotgun approach.

Shotgun proteomics

Digestion, data acquisition and analysis

Each sample was re-suspended in 50 µL 100 mM ammonium bicarbonate (Sigma Aldrich, Overijse, Belgium) buffer (pH 7.8). Proteins were then denatured, reduced, alkylated and

digested overnight and finally reaction was stopped, samples evaporated and re-suspended in 100 µL 0.1% aqueous formic acid (v/v) prior to analysis as earlier described (Delporte et al., 2014). Ten microliters of the digested samples were injected into the LC-system. Analyses were performed with a rapid resolution liquid chromatograph (RRLC) in reversed phase mode coupled to an electrospray ion source - quadrupole time-of-flight (Q-TOF) for the MS and auto MS/MS analyses, using the same parameters as in (Delporte et al., 2014). Data were acquired by the Mass Hunter Acquisition® software (version B.04 patch 3, Agilent Technologies) and analyzed by the Spectrum Mill® Workbench software (Rev B.04.01.141, Agilent Technologies) with the last updated UniProt (Swiss-Prot, November, 2016) database. Peptides and proteins were identified and validated using parameters described in (Delporte et al., 2014). Samples were injected three times in MS mode and once in autoMS/MS mode. For chemometrics and statistical analysis, LC-MS data were converted from .d format (Agilent) to either .mzXML (MS Converter from ProteoWizard) or .mzData type (exported by MH Qual, Agilent Software).

Multivariate data analysis

For the unsupervised and supervised multivariate analyses, the data obtained from the LC-MS was considered. Five different treatment conditions, i.e., non-treated control (1), treated with 0.1 (2) or 1.0 µM (3) CM16 for 15 h, or with 0.1 (4) or 1.0 µM (5) CM16 for 24 h, were tested in Hs683 cells in five independent replicates and each replicate was injected three times for LC-MS analysis, totalizing 75 runs. Four outliers were excluded, thus 71 chromatograms were analyzed. The data matrix **X** [m x n] considered for the multivariate analyses consists of n = 71 samples and m = 12701 variables, with the latter representing the number of time points at which a signal intensity was measured (0-105 min). Pre-processing of the data was performed before further analysis. Peak alignment was applied for the 71 samples, using the correlation optimized warping (COW), with the warping toolbox in MatLab (The Mathworks,

MA). Normalization to the internal standard ovalbumin was also performed as described in the formula below:

$$\boldsymbol{S_{norm}} = \left(\frac{\boldsymbol{S_i}}{\sum_{i=1}^{m} S_{isc}}\right) \cdot \boldsymbol{\overline{x}_n}$$

where each normalized sample ($\boldsymbol{S_{norm}}$) was obtained by dividing each original individual chromatogram $\boldsymbol{S_i}$ at each condition by the sum of the internal standard chromatogram (extracted ion chromatogram of ovalbumin) added to each condition ($\sum_{i=1}^{m} S_{isc}$), where m is the peak intensity measured for each time point ($m = 1 \ldots 12701$) multiplied by the average sum $\boldsymbol{\overline{x}_n}$ of the n 71 internal standard chromatograms.

Unsupervised principal component analysis (PCA) allows visualizing the information contained in the matrix **X** in a new space, represented by principal components (PC's), which are linear combinations of the original variables. The contribution of each original variable to a PC is given by its loading. *Hierarchical Clustering Analysis* (HCA) also allows visualization of (dis)similarity among samples that were merged in clusters based on a distance, e.g. the Euclidean distance in the present study. The objects linked first are the most similar and clustering continues until all samples are clustered (Klein-Júnior et al., 2016). PCA and HCA analyses were performed to investigate whether the source of variance in the samples could be attributed, at least partly, to CM16 treatment. Both analyses were performed in MatLab with the ChemoAC v. 4.1 toolbox.

Supervised analysis for classification was made with SIMCA (Soft Independent Modeling by Class Analogy), in which PCA models are created for each class individually (Smit et al., 2009). The entire data set was applied as calibration set and models were evaluated based on cross validation by leave-more-out with Venetian blinds as well as by the calculation of class sensitivity and specificity (ratio). Three PCs were selected to model classes 1 (controls) and 5

(1 μM CM16 for 24h), four PCs to model classes 2 and 3 (0.1 μM CM16 for 15 and 24h respectively), and five to model class 4 (1 μM CM16 for 15h).

Two-dimensional electrophoresis (2-DE)

Sample loading, 2-DE PAGE, spot detection and protein identification

The protocol described below is an adaptation of Berkelman and Stenstedt (Berkelman & Stenstedt, 1998). Briefly, following precipitation of 3 mg of protein per sample, samples were solubilized in rehydration buffer (7 M urea; 2 M thiourea; 2% CHAPS; 20 mM DTT; 0.5% IPG buffer pH 3–10 NL) and proteins were quantified with a Pierce detergent compatible Bradford assay kit (Thermo Scientific, Leuven, Belgium). A volume of 340 μL rehydration buffer containing 1 mg proteins was used to hydrate the Immobiline DryStrip gels (18 cm, pH 3-10, NL) overnight at room temperature. The isoelectric focusing (IEF) was performed at 20 °C in a Multiphor II system (GE Healthcare, Diegem, Belgium) using a step-wise voltage ramp according to the manufacturer's instructions. After IEF, proteins were reduced and alkylated by incubation with agitation in two equilibrium buffers (6 M urea, 50 mM Tris-HCl, pH 8.8, 30% glycerol, 2% SDS) containing 1% DTT (w/v) and 2.5% iodoacetamide (w/v), respectively. Equilibrated strips were then applied onto 12.5 % SDS-PAGE and the proteins were separated in the second dimension in a Protean II multi-cell system (Bio-Rad, Temse, Belgium).

Proteins were visualized by Coomassie Brilliant Blue R-250 staining. Gels were scanned on a GS-800 (BioRad, Temse, Belgium) and protein spots were analyzed quantitatively using the PDQuest software v. 8.0 build 035 (BioRad, Temse, Belgium). The selection of the spots for sequencing and identification by mass spectrometry was made on the basis of a two fold change and/or a significant t-test analysis ($p < 0.05$) of their densitometry. The selected protein spots were digested in-gel with sequencing grade trypsin (Promega, Leiden, The

Netherlands) and analyzed by mass spectrometry as previously described (Nguyen, Volkov, Vandenbussche, Tompa, & Pauwels, 2018). Based on the peptide sequences, the protein was identified using the MASCOT Sequence Query. In the sequence query search parameters, a MS/MS tolerance of 0.6 Da and only one missed cleavage was allowed per peptide. Cysteine carbamidomethylation and methionine oxidation were also taken into account. The criterion for acceptance of protein identification was a score above the MASCOT threshold, set at a significance level of $p < 0.05$.

Results

Unsupervised analysis of the proteome of glioma cells under CM16 treatment

Given the effects of CM16 on the protein synthesis of cancer cells (Carvalho et al., 2017), we first investigated how the whole proteome of glioma cells was affected by this treatment. Therefore, we used an LC-MS and MS-MS shotgun proteomic approach on the Hs683 human glioma model left untreated or treated with CM16 at 0.1 µM (IC_{50} concentration as determined by means of the MTT assay over 72h, (Carvalho et al., 2017)) or 1 µM (10 times higher concentration) for 15 and 24h. The 309 proteins that we were able to identify and were possibly present in whole Hs683 cell extracts of the different conditions were classified according to their localization, biological and molecular functions (Fig. S1). Briefly, all cell compartments are represented and samples are enriched in proteins involved in their own biogenesis, including ribosome-related and RNA-binding proteins, folding and metabolism.

To conduct unsupervised multivariate analysis on those data, we first reduced dimensionality, by condensing the complex MS data obtained at each retention time into a fingerprint total ion current – TIC chromatogram. Fig. 1b shows the overlay of the mean TICs of each experimental condition.

Thanks to *Hierarchical Clustering Analysis* that groups the samples into clusters based on the Euclidean distance, we observed a high similarity between the three injections of each sample, and a tendency of the TICs to group according to the treatment concentration (Fig. 2a). Indeed, most of the 1 µM treated samples (thicker bars) grouped into one cluster at the right of the tree while most of the negative controls and samples treated with the low concentration (0.1 µM) are grouped into one cluster on the left of the tree.

The TIC data were then submitted to *Principal Component Analysis* (PCA). The PC2-PC3 plot allowed distinction between the treatment conditions even if they account together for

only ~1% of the overall variation in the data (Fig. 2b). This means that while the treatments induced limited changes to the whole proteome of the cells during the first 24h of treatment, those changes can be detected using an LC-MS approach. Considering that CM16 is a cytostatic agent used here over short periods (i.e. 15h and 24h) and that changes in the proteome depend not only on the protein synthesis process but also on gene expression, protein half-life, recycling, and degradation (Chen, Smeekens, & Wu, 2016) it is not surprising that the effects induced by CM16 treatment contributed to such few variation of the data.

To further evaluate the distinction between treated and non-treated samples, we compared the TICs of the non-treated and treated samples by drawing effect plots. Those are obtained by subtracting the average treated-cell TIC profile from the average untreated-cell TIC profile. Applying Dong's algorithm (Vander Heyden, Nijhuis, Smeyers-Verbeke, Vandeginste, & Massart, 2001), we set an error threshold above or below which the effects can be considered significant (Klein-Júnior et al., 2016). Significant effects appear to be time and concentration-dependent (Fig. 2c and Fig. S2). Additionally, we observed some similarities between the significant changes exceeding the critical margins of the difference TIC profiles and the PC2 and PC3 loadings: the peaks detected around 20 min on the differential TIC profile of cells treated with 1µM for 15h (see arrows on Fig. 2c) contribute to the PC2 loadings (Fig. 2d) while those identified in the region between 60 and 80 min seem to contribute to the PC3 loadings (Fig. 2e). Thus, the effect plots and the PC2 and PC3 loadings show certain specific peaks of the original variables that are different between CM16 treated and untreated samples.

Sensitive shotgun MS approach to discriminate CM16 treatment conditions of glioma cells

SIMCA supervised analysis and modelling were then used to investigate the possibility to properly classify the samples according to their treatment on the basis of LC-MS data. SIMCA is a technique that selects a number of principal components to model each experimental treatment, named class, individually. Cross validated classification of the model assigned 61 of 71 injections to the correct class (Table 1). The success rate of 86% confirms that the model was indeed able to correctly classify most samples. Importantly, the non-treated control (class 1) had no misclassification, i.e. no control sample was classified as treated (Table 1). Misclassifications (n=10/ 71) occurred mainly between treatment concentrations or between samples treated by the same CM16 concentration but for different periods of time. Interestingly, five misclassifications occurred between class 3 (15 h - 1µM) and class 5 (24 h - 1µM), which agrees with the results from the unsupervised analysis, in which the two treatment conditions at 1µM clustered together (Fig. 2a).

Thus the gel-free approach appeared sensitive enough to detect that the cytostatic agent CM16 induces significant minimal changes in the proteome of glioma cells, even after a short incubation period, e.g. 15 h. Although the proteomic variation induced by CM16 is significant in both unsupervised and supervised analyses, the complexity of the data contained in the TICs profiles did not allow us to identify specific proteins, whose expression are affected by CM16.

CM16 treatment affects the expression of specific proteins involved in protein synthesis and aggressiveness of glioma cells

To analyze CM16-induced effects on the protein expression profile of Hs683 cells, we thus moved to classical 2D electrophoresis. Untreated glioma cells were compared with CM16 treated ones for 15h at 1µM, the latter condition having been selected on the basis of the

earliest time point showing a marked differential TIC profile in the LC-MS analysis (Fig. 2c and Fig. S2). Representative gels of each condition are provided in Fig. S3. An average of 357 spots per gel was detected with a matching rate ranging from 53 to 97% between gels corresponding to a correlation coefficient of about 0.7. According to the applied cut-off (two-fold change and/or $p < 0.05$ from t-test analysis), eight spots showed significant changes in CM16-treated cells compared to the non-treated glioma cells (Fig. S3).

These spots were cut and analyzed through MS and MS/MS. Eight proteins were assigned to the 8 spots as follows: HspB1 (heat shock protein beta-1), Ebp1 (ErbB3-binding protein 1), PGAM1 (Phosphoglycerate mutase 1), CK-18 (cytokeratin-18), transcription factor BTF3, galectin-1, cofilin and dUTPase (Table 2, with their respective recovery rates). Two were upregulated, i.e. galectin-1 and Ebp1, while the other six were downregulated (see table 2). When searching for those specific proteins in the LC-MS data, four of them could be retrieved: HspB1, cofilin, PGAM1 and keratin 18 (Table 2, highlighted in grey). Importantly, they displayed the same trend (up/downregulation) as verified by relative quantification of the peptides analyzed (data not shown).

In order to address the possible molecular interactions among these eight proteins as well as the initiation factors highlighted in the previous study - *EIF1AX*, *EIF3E* and *EIF3H* gene products and eIF2α - (Carvalho et al., 2017), the STRING tool was used. This database collects information of protein-protein association from different sources which enables to map out interactions of physical and functional types that are biologically meaningful for the proteins of interest (Deutsch, Lam, & Aebersold, 2008; Szklarczyk et al., 2017). Analysis of the functional enrichment in the network of the twelve proteins showed enrichment of ten of these proteins for only one annotation, i.e. RNA binding (Fig. 3). Interestingly these twelve proteins were identified in a large study defining the mRNA interactome of HeLa cells as possible RNA-binding proteins (RBPs), yet to be validated (Castello et al., 2012). RBPs are

associated with RNAs throughout their entire life cycle and participate in many functions from RNA synthesis to decay (Castello et al., 2012). Moreover, the eight proteins found in the 2-D gel based approach play various roles in cancer as discussed below, with respect to their specific roles in glioma biology. Therefore the fact that they appear to be down or upregulated in Hs683 glioma cells when treated with CM16 could help understanding how this compound displays some selectivity towards cancer cells as earlier reported (Carvalho et al., 2017).

Discussion

Harmine cannot be used as such for its anti-cancer properties because of its neurotoxicity (Cao et al., 2004; Chen et al., 2004) but its scaffold is still of great interest for drug development. By example a N2-benzylated β-carboline derivative was recently shown to trigger apoptosis through PI3K/Akt inhibition and ROS production provoking thereby tumor growth inhibition in a colorectal cancer model *in vivo* (Zhang et al., 2016). Also trisubstituted β-carbolines appear promising with some of them having already been described to display antiproliferative effects both *in vitro* and *in vivo* , notably in lung cancer and sarcoma bearing mice with low acute toxicity (Zhang et al., 2013). We previously reported CM16 as another trisubstituted harmine derivative with potent cytostatic protein synthesis inhibitory properties on cancer cells (Carvalho et al., 2017). We herein conducted a proteomic investigation to gain further insight into its anti-cancer effects in glioma cells. Proteomics in cancer research has been successfully applied in the search for biomarkers as well as in drug target discovery (Dias, Kitano, Zelanis, & Iwai, 2016).

In this study, the shotgun approach appeared sensitive enough to discriminate the treated from the untreated cells by both unsupervised and supervised analyses even when the variations induced by the treatments did not account for more than 1% of the total variation among the samples (Fig. 2b). However, the identification of specific proteins involved in the changes

observed in TIC profile was not possible due to the reduction of the data. Moreover, evaluation of low-abundance proteins is limited with shotgun proteomics due to the dynamic range of protein concentrations (Matallana-Surget, Leroy, & Wattiez, 2010). This could, for instance, be the case with respect to the *EIF1AX*, *EIF3E* and *EIF3H* gene products that we identified previously through transcriptomic analysis as possible drivers of cancer cell sensitivity to CM16 (Carvalho et al., 2017). We thus used also the 2-DE-gel-based conventional approach to identify differentially expressed proteins under CM16 treatment. Among these, the heat shock protein beta-1 (HspB1 or, alternatively, HSP 27), is induced in stress conditions and works as a molecular chaperone, conferring protection against protein misfolding (Arrigo & Gibert, 2013). Because of its chaperone role, HspB1 interacts with a variety of proteins involved in cancer cell growth, migration, transcription, translation, apoptosis and senescence suppression (Arrigo & Gibert, 2013). Inhibiting HspB1 leads to decrease in proliferation, migration and invasion of cancer cells as already shown with anticancer drugs such as imatinib and actinomycin D (Wu et al., 2017). Moreover, HspB1 also modulates chemotherapeutic drug resistance and is related to poor prognosis in cancer (Wu et al., 2017). Accordingly, although it is constitutively expressed in most tissues, HspB1 expression increases with World Health Organization (WHO) grading of astrocytic glioma (Mäkelä et al., 2014) and is correlated with poor survival of glioma patients (Gimenez et al., 2015). Furthermore, it has been associated with resistance to temozolomide *in vivo* (Jakubowicz-Gil, Langner, Bądziul, Wertel, & Rzeski, 2013), making CM16 a possible good candidate to be used in combination to overcome this chemoresistance. Importantly, HspB1 has also been associated to translation inhibition by its capacity to bind eIF4G, preventing thereby the assembly of the eIF4F complex required for cap-dependent protein synthesis (Cuesta, Laroia, & Schneider, 2000). Further investigations should be conducted to determine

whether the possible HspB1 downregulation observed after CM16 treatment is confirmed and contributes to its antiproliferative and protein synthesis inhibitory activity.

Similarly, CM16 decreases the expression levels of the transcription factor BTF3 (alternatively, NAC-beta). The name "NAC-beta" relates to its interaction with the nascent polypeptide chain coming from the ribosomes (Kogan & Gvozdev, 2014). In addition, BTF3 is a RNA polymerase II transcription factor involved in apoptosis and cell cycle regulation (Kusumawidjaja et al., 2007), as well as in the endoplasmic reticulum biogenesis (Roy et al., 2010). Thus, the downregulation of BTF3, caused by CM16 in glioma cells, might also contribute to its protein synthesis inhibition effect. Interestingly, BTF3 is overexpressed in high grade glioma (Odreman et al., 2005) and is suggested to be among the top 10 key genes for glioblastoma development (Kunkle, Yoo, & Roy, 2013).

PGAM1 is an enzyme participating in glycolysis by converting 3-PG (3-phosphoglycerate) to 2-PG (Fothergill-Gilmore & Watson, 1990) whose expression also correlates with glioma grade and patient survival (Gao et al., 2013). Although its role in cancer is still poorly understood, its knockdown increases the survival of glioblastoma bearing mice (Sanzey et al., 2015). PGAM1 downregulation appeared thus as an interesting possible event triggered by CM16 to combat glioma.

Other interesting results concern the decrease in mitochondrial dUTPase and cofilin. dUTPase catalyzes the transformation of dUTP into dUMP, eliminating the excess of dUTP and avoiding thereby its incorporation into the DNA. When incorporated, dUTP causes double-stranded DNA breaks leading to cell death (Vertessy & Toth, 2009). Thus, further validation of CM16-induced decrease in dUTPase may be needed to possibly envisage its use for sensitizing cancer cells to DNA targeting chemotherapeutic agents as already proposed with respect to 5-FU (Ladner et al., 2000).

Cofilin downregulation induced by CM16 might confer additional anti-migratory properties to its cytostatic effects. Indeed, this actin filament assembly and disassembly regulator plays an important role in cell migration (Bernstein & Bamburg, 2010) and is overexpressed in glioblastoma (Naryzhny et al., 2014). The effects of CM16 on those five proteins seem thus promising when considering their roles in glioma biology as confirmed by the benefits obtained with their inhibition in glioma models, exemplified by the literature reported here.

Finally, two upregulated proteins were identified in Hs683 cells treated with CM16, i.e. galectin-1 (Gal1) and the proliferation-associated protein 2G4 (Ebp1). Gal1 is overexpressed in numerous cancer types, including all types of human gliomas, where it is involved in cancer progression and poor prognosis (Le Mercier, Fortin, Mathieu, Kiss, & Lefranc, 2010). Gal1 expression has been shown to increase after radiotherapeutic and chemotherapeutic insults. Because Gal1 has also been reported to be part of the spliceosome, participating in the pre-mRNA splicing before its translation (Haudek, Patterson, & Wang, 2010), possible up-regulation of Gal1 by CM16 may be hypothesized as a cancer cell defense mechanism in link with this later function. The other up-regulated protein is the Ebp1, known to promote cell survival and prevent apoptosis by associating with Akt (Ko, Chang, Park, & Ahn, 2016). Accordingly, high Ebp1 levels have been associated with poor clinical outcome of glioblastoma patients (Ko et al., 2016). Interestingly, Ebp1 is also known to inhibit phosphorylation of eukaryotic initiation factor 2α (eIF2α), thus allowing translation to occur (Squatrito, Mancino, Sala, & Draetta, 2006). Given that we previously reported induction of eIF2α phosphorylation by CM16 in a breast cancer cell model (Carvalho et al., 2017), possible up-regulation of Ebp1 might also be envisaged as a consequent defense of the cancer cell. These hypotheses remain however to be investigated at the cellular and molecular levels.

In conclusion, this proteomic study revealed that CM16 induces significant changes in the proteome of glioma cells in a time- and concentration- dependent manner. In particular, this study showed that CM16 decreases the expression of five proteins associated with glioma aggressiveness and poor clinical outcome. On the contrary, the two upregulated proteins identified might be linked to defense mechanisms of the cells to CM16 insult. Importantly, HspB1 and Ebp1 are actively participating in protein synthesis regulation, together with the initiation factors *EIF1AX*, *EIF3E* and *EIF3H* and eIF2α (Fig. 3) identified in the previous study as possible relevant cell components for CM16 responsiveness (Carvalho et al., 2017), while BTF3 and Gal1 may be indirectly involved. Further investigations are required to validate whether CM16 treatment actually change the protein expression level and/ or activation status of those possible different actors identified by transcriptomic and proteomic studies. In addition, we intend to decipher each of their role(s) in CM16 anti-proliferative effects by silencing techniques to pursue our investigations of this harmine derivative as a protein synthesis inhibitor to combat glioma.

Acknowledgments

The PhD of A.C. has been financially supported by the Coordenação de Aperfeiçoamento de Pessoal de Nível Superior (Grant 0674-13/3; CAPES; Brazil). Part of this study has also been supported by the grant by the Belgian Brain Tumor Support (BBTS; Belgium), the Belgian National Fund for Scientific Research (FRS, N° 3.4553.08 and T.0136.13 PDR), and the Université Libre de Bruxelles (FER-207). FS is particularly thankful to UGA (Grenoble) for the scientific delegation conceded at Faculty of Pharmacy ULB (Brussels) and in particular Prof C. Ribuot and Prof E. Peyrin.

Conflict of interest

The authors declare that they have no conflict of interest.

References

Arrigo, A.-P., & Gibert, B. (2013). Protein interactomes of three stress inducible small heat shock proteins: HspB1, HspB5 and HspB8. *International Journal of Hyperthermia*, *29*(5), 409–422. doi:10.3109/02656736.2013.792956

Azad, T. D., Pan, J., Connolly, I. D., Remington, A., Christy, M., & Grant, G. A. (2015). Therapeutic strategies to improve drug delivery across the blood-brain barrier. *Neurosurgery Focus*, *38*(3), 1–19.

Beier, D., Schulz, J. B., & Beier, C. P. (2011). Chemoresistance of glioblastoma cancer stem cells - much more complex than expected. *Molecular Cancer*, *10*(1), 1–11. doi:10.1186/1476-4598-10-128

Berkelman, T., & Stenstedt, T. T. (1998). *2-D Electrophoresis using immobilized pH gradients - Principles and Methods*. *Amersham Biosciences*. Uppsala: Amersham Biosciences.

Bernstein, B. W., & Bamburg, J. R. (2010). ADF/Cofilin: A functional node in cell biology. *Trends in Cell Biology*, *20*(4), 187–195. doi:10.1016/j.tcb.2010.01.001

Bhat, M., Robichaud, N., Hulea, L., Sonenberg, N., Pelletier, J., & Topisirovic, I. (2015). Targeting the translation machinery in cancer. *Nature Reviews Drug Discovery*, *14*(4), 261–278. doi:10.1038/nrd4505

Cao, R., Chen, Q., Hou, X., Chen, H., Guan, H., Ma, Y., … Xu, A. (2004). Synthesis, acute toxicities, and antitumor effects of novel 9-substituted β-carboline derivatives. *Bioorganic and Medicinal Chemistry*, *12*(17), 4613–4623. doi:10.1016/j.bmc.2004.06.038

Cao, R., Guan, X., Shi, B., Chen, Z., Ren, Z., Peng, W., & Song, H. (2010). Design, synthesis and 3D-QSAR of beta-carboline derivatives as potent antitumor agents. *European Journal of Medicinal Chemistry*, *45*(6), 2503–2515. doi:10.1016/j.ejmech.2010.02.036

Cao, R., Peng, W., Chen, H., Ma, Y., Liu, X., Hou, X., … Xu, A. (2005). DNA binding properties of 9-substituted harmine derivatives. *Biochemical and Biophysical Research Communications*, *338*(3), 1557–1563. doi:10.1016/j.bbrc.2005.10.121

Carvalho, A., Chu, J., Meinguet, C., Kiss, R., Vandenbussche, G., Masereel, B., … Mathieu, V. (2017). Harmine-derived beta-carboline displays anti-cancer effects in vitro by targeting protein synthesis of cancer cells. *European Journal of Pharmacology*, *805*, 25–35. doi:10.1016/j.ejphar.2017.03.034

Castello, A., Fischer, B., Eichelbaum, K., Horos, R., Beckmann, B. M., Strein, C., … Hentze, M. W. (2012). Insights into RNA Biology from an Atlas of Mammalian mRNA-Binding Proteins. *Cell*, *149*(6), 1393–1406. doi:10.1016/j.cell.2012.04.031

Chen, Q., Chao, R., Chen, H., Hou, X., Yan, H., Zhou, S., … Xu, A. (2004). Antitumor and neurotoxic effects of novel harmine derivatives and structure-activity relationship analysis. *International Journal of Cancer*, *114*, 675–682. doi:10.1002/ijc.20703

Chen, W., Smeekens, J. M., & Wu, R. (2016). Systematic study of the dynamics and half-lives of newly synthesized proteins in human cells. *Chemical Science*, *7*(2), 1393–1400. doi:10.1039/C5SC03826J

Cuesta, R., Laroia, G., & Schneider, R. J. (2000). Chaperone Hsp27 inhibits translation during heat shock by binding eIF4G and facilitating dissociation of cap-initiation complexes. *Genes and Development*, *14*(12), 1460–1470. doi:10.1101/gad.14.12.1460

Dai, F., Chen, Y., Song, Y., Huang, L., Zhai, D., Dong, Y., … Yi, Z. (2012). A Natural Small Molecule Harmine Inhibits Angiogenesis and Suppresses Tumour Growth through Activation of p53 in Endothelial Cells. *PLoS ONE*, *7*(12), e52161. doi:10.1371/journal.pone.0052162

Delporte, C., Boudjeltia, K. Z., Noyon, C., Furtmüller, P. G., Nuyens, V., Slomianny, M.-C., … Van Antwerpen, P. (2014). Impact of myeloperoxidase-LDL interactions on enzyme

activity and subsequent posttranslational oxidative modifications of apoB-100. *Journal of Lipid Research*, *55*(4), 747–57. doi:10.1194/jlr.M047449

Deutsch, E. W., Lam, H., & Aebersold, R. (2008). Data analysis and bioinformatics tools for tandem mass spectrometry in proteomics. *Gene Expression*, *33*, 18–25. doi:10.1152/physiolgenomics.00298.2007.

Dias, M. H., Kitano, E. S., Zelanis, A., & Iwai, L. K. (2016). Proteomics and drug discovery in cancer. *Drug Discovery Today*, *21*(2), 264–277. doi:10.1016/j.drudis.2015.10.004

Fothergill-Gilmore, L. A., & Watson, H. C. (1990). Phosphoglycerate mutases. *Biochemlcal Society Transactions*, *18*, 190–193.

Frosina, G. (2009). DNA repair and resistance of gliomas to chemotherapy and radiotherapy. *Molecular Cancer Research : MCR*, *7*(7), 989–99. doi:10.1158/1541-7786.MCR-09-0030

Gao, H., Yu, B., Yan, Y., Shen, J., Zhao, S., Zhu, J., … Gao, Y. (2013). Correlation of expression levels of ANXA2, PGAM1, and CALR with glioma grade and prognosis. *Journal of Neurosurgery*, *118*(4), 846–53. doi:10.3171/2012.9.JNS112134

Gimenez, M., Marie, S. K. N., Oba-Shinjo, S., Uno, M., Izumi, C., Oliveira, J. B., & Rosa, J. C. (2015). Quantitative proteomic analysis shows differentially expressed HSPB1 in glioblastoma as a discriminating short from long survival factor and NOVA1 as a differentiation factor between low-grade astrocytoma and oligodendroglioma. *BMC Cancer*, *15*(481), 1–13. doi:10.1186/s12885-015-1473-9

Görg, A., Obermaier, C., Boguth, G., Harder, A., Scheibe, B., Wildgruber, R., & Weiss, W. (2000). The current state of two-dimensional electrophoresis with immobilized pH gradients. *Electrophoresis*, *21*(6), 1037–1053. doi:10.1002/(SICI)1522-2683(20000401)21:6<1037::AID-ELPS1037>3.0.CO;2-V

Guo, L., Ma, Q., Chen, W., Fan, W., Zhang, J., & Dai, B. (2019). Synthesis and biological evaluation of novel N - heterobivalent β -carbolines as angiogenesis inhibitors. *Journal of Enzyme Inhibition and Medicinal Chemistry*, *34*(1), 375–387. doi:10.1080/14756366.2018.1497619

Han, X., Zhang, J., Guo, L., Cao, R., Li, Y., Li, N., … Si, S. (2012). A Series of Beta-Carboline Derivatives Inhibit the Kinase Activity of PLKs. *PLoS ONE*, *7*(10). doi:10.1371/journal.pone.0046546

Haudek, K. C., Patterson, R. J., & Wang, J. L. (2010). SR proteins and galectins: What's in a name? *Glycobiology*, *20*(10), 1199–1207. doi:10.1093/glycob/cwq097

Hershey, J. W. B., Sonenberg, N., & Mathews, M. B. (2012). Principles of Translational Control: An Overview. *Cold Spring Harbor Perspectives in Biology*, *4*, a011528. doi:10.1101/cshperspect.a009829

Itoua Maïga, R., Cencic, R., Chu, J., Waller, D. D., Brown, L. E., Devine, W. G., … Pelletier, J. (2019). Oxo-aglaiastatin-Mediated Inhibition of Translation Initiation. *Scientific Reports*, *9*(1), 1265. doi:10.1038/s41598-018-37666-5

Jakubowicz-Gil, J., Langner, E., Bądziul, D., Wertel, I., & Rzeski, W. (2013). Silencing of Hsp27 and Hsp72 in glioma cells as a tool for programmed cell death induction upon temozolomide and quercetin treatment. *Toxicology and Applied Pharmacology*, *273*(3), 580–9. doi:10.1016/j.taap.2013.10.003

Klein-Júnior, L. C., Viaene, J., Salton, J., Koetz, M., Gasper, A. L., Henriques, A. T., & Vander Heyden, Y. (2016). The use of chemometrics to study multifunctional indole alkaloids from Psychotria nemorosa (Palicourea comb. nov.). Part I: Extraction and fractionation optimization based on metabolic profiling. *Journal of Chromatography A*, *1463*, 60–70. doi:10.1016/j.chroma.2016.07.030

Ko, H. R., Chang, Y. S., Park, W. S., & Ahn, J.-Y. (2016). Opposing roles of the two isoforms of ErbB3 binding protein 1 in human cancer cells. *International Journal of*

Cancer, *139*(6), 1202–1208. doi:10.1002/ijc.30165
Kogan, G. L., & Gvozdev, V. A. (2014). Multifunctional nascent polypeptide-associated complex (NAC). *Molecular Biology*, *48*(2), 189–196. doi:10.1134/S0026893314020095
Kunkle, B. W., Yoo, C., & Roy, D. (2013). Reverse engineering of modified genes by Bayesian network analysis defines molecular determinants critical to the development of glioblastoma. *PloS One*, *8*(5), e64140. doi:10.1371/journal.pone.0064140
Kusumawidjaja, G., Kayed, H., Giese, N., Bauer, A., Erkan, M., Giese, T., … Kleeff, J. (2007). Basic transcription factor 3 (BTF3) regulates transcription of tumor-associated genes in pancreatic cancer cells. *Cancer Biology and Therapy*, *6*(3), 367–376. doi:10.4161/cbt.6.3.3704
Ladner, R. D., Lynch, F. J., Groshen, S., Xiong, Y. P., Sherrod, A., Caradonna, S. J., … Lenz, H. (2000). dUTP Nucleotidohydrolase Isoform Expression in Normal and Neoplastic Tissues: Association with Survival and Response to 5-Fluorouracil in Colorectal Cancer. *Cancer Research*, *60*, 3493–3503.
Le Mercier, M., Fortin, S., Mathieu, V., Kiss, R., & Lefranc, F. (2010). Galectins and gliomas. *Brain Pathology*, *20*(1), 17–27. doi:10.1111/j.1750-3639.2009.00270.x
Li, S., Wang, A., Gu, F., Wang, Z., Tian, C., Qian, Z., … Gu, Y. (2015). Novel harmine derivatives for tumor targeted therapy. *Oncotarget*, *6*(11), 8988–9001.
Luo, W., Liu, J., Li, J., Zhang, D., Liu, M., Addo, J. K., … Huang, C. (2008). Anti-cancer effects of JKA97 are associated with its induction of cell apoptosis via a Bax-dependent and p53-independent pathway. *Journal of Biological Chemistry*, *283*(13), 8624–8633. doi:10.1074/jbc.M707860200
Ma, Q., Chen, W., & Chen, W. (2016). Anti-tumor angiogenesis effect of a new compound: B-9-3 through interference with VEGFR2 signaling. *Tumor Biology*, *37*(5), 6107–6116. doi:10.1007/s13277-015-4473-0
Mäkelä, K. S., Haapasalo, J. A., Ilvesaro, J. M., Parkkila, S., Paavonen, T., & Haapasalo, H. K. (2014). Hsp27 and its expression pattern in diffusely infiltrating astrocytomas. *Histology and Histopathology*, *29*(9), 1161–8. doi:10.14670/HH-29.1161
Masuia, K., Caveneeb, W. K., & Mischel, P. S. (2016). Cancer metabolism as a central driving force of glioma pathogenesis. *Brain Tumor Pathology*, *33*, 161–168. doi:10.1007/s10014-016-0265-5
Matallana-Surget, S., Leroy, B., & Wattiez, R. (2010). Shotgun proteomics: concept, key points and data mining. *Expert Review of Proteomics*, *7*(1), 5–7. doi:10.1586/epr.09.101
Meinguet, C., Bruyère, C., Frédérick, R., Mathieu, V., Vancraeynest, C., Pochet, L., … Wouters, J. (2015). 3D-QSAR, Design, Synthesis and characterization of trisubstituted harmine derivatives with in vitro antiproliferative properties. *European Journal of Medicinal Chemistry*, *94*, 45–55. doi:10.1016/j.ejmech.2015.02.044
Naryzhny, S. N., Ronzhina, N. L., Mainskova, M. A., Belyakova, N. V., Pantina, R. A., & Filatov, M. V. (2014). Development of barcode and proteome profiling of glioblastoma. *Biochemistry (Moscow) Supplement Series B: Biomedical Chemistry*, *8*(3), 243–251. doi:10.1134/S1990750814030111
Nguyen, H. H., Volkov, A. N., Vandenbussche, G., Tompa, P., & Pauwels, K. (2018). In vivo biotinylated calpastatin improves the affinity purification of human m-calpain. *Protein Expression and Purification*, *145*, 77–84. doi:10.1016/j.pep.2018.01.002
Odreman, F., Vindigni, M., Gonzales, M. L., Niccolini, B., Candiano, G., Zanotti, B., … Vindigni, A. (2005). Proteomic studies on low- and high-grade human brain astrocytomas. *Journal of Proteome Research*, *4*(3), 698–708. doi:10.1021/pr0498180
Ostrom, Q. T., Bauchet, L., Davis, F. G., Deltour, I., Fisher, J. L., Langer, C. E., … Barnholtz-Sloan, J. S. (2014). The epidemiology of glioma in adults: A state of the science review. *Neuro-Oncology*, *16*(7), 896–913. doi:10.1093/neuonc/nou087

Paw, I., Carpenter, R. C., Watabe, K., Debinski, W., & Lo, H.-W. (2015). Mechanisms regulating glioma invasion. *Cancer Letters*, *362*(1), 1–7. doi:10.1016/j.canlet.2015.03.015

Pozo, N., Zahonero, C., Fernández, P., Liñares, J. M., Ayuso, A., Hagiwara, M., … Sánchez-Gómez, P. (2013). Inhibition of DYRK1A destabilizes EGFR and reduces EGFR-dependent glioblastoma growth. *Journal of Clinical Investigation*, *123*(6), 2475–2487. doi:10.1172/JCI63623

Radhakrishnan, A., Nanjappa, V., Raja, R., Sathe, G., Puttamallesh, V. N., Jain, A. P., … Chatterjee, A. (2016). A dual specificity kinase, DYRK1A, as a potential therapeutic target for head and neck squamous cell carcinoma. *Scientific Reports*, *6*(1), 36132. doi:10.1038/srep36132

Roy, L., LaBoissière, S., Abdou, E., Thibault, G., Hamel, N., Taheri, M., … Paiement, J. (2010). Proteomic analysis of the transitional endoplasmic reticulum in hepatocellular carcinoma: An organelle perspective on cancer. *Biochimica et Biophysica Acta - Proteins and Proteomics*, *1804*(9), 1869–1881. doi:10.1016/j.bbapap.2010.05.008

Ruggero, D. (2013). Translational Control in Cancer Etiology. *Cold Spring Harbor Perspectives in Biology*, *5*, a012336. doi:10.1101/cshperspect.a015891

Sanzey, M., Abdul Rahim, S. A., Oudin, A., Dirkse, A., Kaoma, T., Vallar, L., … Niclou, S. P. (2015). Comprehensive analysis of glycolytic enzymes as therapeutic targets in the treatment of glioblastoma. *PloS One*, *10*(5), e0123544. doi:10.1371/journal.pone.0123544

Seifert, A., Allan, L. A., & Clarke, P. R. (2008). DYRK1A phosphorylates caspase 9 at an inhibitory site and is potently inhibited in human cells by harmine. *FEBS Journal*, *275*(24), 6268–6280. doi:10.1111/j.1742-4658.2008.06751.x

Smit, S., Govorukhina, N. I., Hoefsloot, H. C. J., Horvatovich, P. L., Suits, F., Zee, A. van der, … Smilde, A. K. (2009). Enhancing classification performance: covariance matters. In S. Smit (Ed.), *Statistical data processing in clinical proteomics* (pp. 81–92). Amsterdam: UvA-DARE (Digital Academic Repository) Statistical.

Squatrito, M., Mancino, M., Sala, L., & Draetta, G. F. (2006). Ebp1 is a dsRNA-binding protein associated with ribosomes that modulates eIF2α phosphorylation. *Biochemical and Biophysical Research Communications*, *344*(3), 859–868. doi:10.1016/j.bbrc.2006.03.205

Strickland, M., & Stoll, E. A. (2017). Metabolic Reprogramming in Glioma. *Frontiers in Cell and Developmental Biology*, *5*(43), 1–32. doi:10.3389/fcell.2017.00043

Strong, J. M., Garces, J., Vera, J. C., Mathkour, M., Emerson, N., & Ware, M. L. (2015). Brain Tumors: Epidemiology and Current Trends in Treatment. *Journal of Brain Tumors & Neurooncology*, *1*(1), 1–21. doi:10.4172/2475-3203.1000102

Szklarczyk, D., Morris, J. H., Cook, H., Kuhn, M., Wyder, S., Simonovic, M., … von Mering, C. (2017). The STRING database in 2017: quality-controlled protein–protein association networks, made broadly accessible. *Nucleic Acids Research*, *45*(D1), D362–D368. doi:10.1093/nar/gkw937

Vander Heyden, Y., Nijhuis, A., Smeyers-Verbeke, J., Vandeginste, B. G. M., & Massart, D. L. (2001). Guidance for robustness/ruggedness tests in method validation. *Journal of Pharmaceutical and Biomedical Analysis*, *24*(5–6), 723–753. doi:10.1016/S0731-7085(00)00529-X

Vertessy, B. G., & Toth, J. (2009). Keeping uracil out of DNA: physiological role, structure and catalytic mechanism of dUTPases. *Accounts of Chemical Research*, *42*(1), 97–106. doi:10.1021/ar800114w

Wu, J., Liu, T., Rios, Z., Mei, Q., Lin, X., & Cao, S. (2017). Heat Shock Proteins and Cancer. *Trends in Pharmacological Sciences*, *38*(3), 226–256. doi:10.1016/j.tips.2016.11.009

Xie, J., Merrett, J. E., Jensen, K. B., & Proud, C. G. (2019). The MAP kinase-interacting kinases (MNKs) as targets in oncology. *Expert Opinion on Therapeutic Targets*, *16*, 1–13. doi:10.1080/14728222.2019.1571043

Zhang, G., Cao, R., Guo, L., Ma, Q., Fan, W., Chen, X., … Ren, Z. (2013). Synthesis and structure-activity relationships of N2-alkylated quaternary beta-carbolines as novel antitumor agents. *European Journal of Medicinal Chemistry*, *65*, 21–31. doi:10.1016/j.ejmech.2013.04.031

Zhang, H., Sun, K., Ding, J., Xu, H., Zhu, L., Zhang, K., … Sun, W. (2014). Harmine induces apoptosis and inhibits tumor cell proliferation, migration and invasion through down-regulation of cyclooxygenase-2 expression in gastric cancer. *Phytomedicine*, *21*(3), 348–355. doi:10.1016/j.phymed.2013.09.007

Zhang, X.-F., Sun, R., Jia, Y., Chen, Q., Tu, R.-F., Li, K., … Cao, R. (2016). Synthesis and mechanisms of action of novel harmine derivatives as potential antitumor agents. *Scientific Reports*, *6*(1), 33204. doi:10.1038/srep33204

Table 1 Supervised SIMCA classification results, sensitivity and specificity attributed to each class (experimental condition).

Class number	Type of samples	Number of samples	Correct classification (Cross validation)	Sensitivity	Specificity
1	CT – Non-treated	15	15	1.00	0.98
2	15h - 0.1 µM	15	13	0.87	1.00
3	15h - 1.0 µM	15	13	0.87	0.95
4	24h - 0.1 µM	14	10	0.71	1.00
5	24h - 1.0 µM	12	10	0.83	0.90
Total		71	61	-	-

Table 2 Proteins identified in the gel-based approach (2-DE), their regulation and information from sequencing. Proteins highlighted in grey were also found in the shotgun approach dataset.

Protein name	Regulation in CM16 treated Hs683 cells	Swiss-Prot ID	Mass (kDa)/pI	Mascot score (sequence query search)	% C (sequence coverage)
Heat shock protein beta-1	down	P04792	22.78/5.98	779	75
Cofilin-1	down	P23528	18.50/8.22	264	59
Transcription factor BTF3	down	P20290	22.17/9.41	785	53
Phosphoglycerate mutase 1	down	P18669	28.80/6.67	492	45
Galectin-1	up	P09382	14.71/5.34	284	38
Keratin, type I cytoskeletal 18	down	P05783	48.06/534	790	42
Deoxyuridine 5'-triphosphate nucleotidohydrolase, mitochondrial	down	P33316	26.56/9.46	405	26
Proliferation-associated protein 2G4/ Ebp1	up	Q9UQ80	43.79/6.13	767	29

Legends to figures

Fig. 1 a chemical structure of CM16. **b** Overlay of the average fingerprint TIC chromatograms of the samples for each condition (Time x Peak intensity) used in the unsupervised and supervised analyses. Outliers were identified visually when looking at the overlapped profiles of each run and excluded for further data analysis (data not shown).

Fig. 2 Results of the unsupervised analysis **a** Dendrograms obtained with the TIC of all conditions with color code attributed to the CM16 treatments. The numbers on the x axis correspond to the samples injected (1-71). The three replicate injections of a sample are clustered together (e.g. 16-17-18 are three injections of one 15 h-1.0 µM sample). **b** PC2-PC3 score plot of the TIC of all conditions with color code attributed to the CM16 treatments. The black, orange and purple ellipses indicate the clustering tendency of the untreated control samples and of those treated with 0.1 µM and 1 µM CM16, respectively. **c** Graphical representation of the effects at each time point (effect plot), presented as the difference between the mean TIC profile of samples treated by CM16 for 15 h at 1 µM and the non-treated samples (horizontal solid lines: critical effect values obtained by Dong's algorithm). **d and e** Loadings of the original variables to PC2 and PC3, respectively. Arrows indicate the peaks on the loadings, detected around 20 min (PC2) and between 60-80 (PC3), that were also indicated as significant effects in the differential TIC profile effect plot in 2c.

Fig. 3 Networking of the twelve genes linked to CM16 effects in cancer cells. Node in red showing the genes identified as enriched for RNA binding. HSPB1, PA2G4 (Ebp1) and the initiation factors seem to directly participate in the protein synthesis regulation. Association of HspB1, dUTPase (DUT) and cofilin 1 (CFL1) and PA2G4, EIF1AX, EIF3E, EIF3H and EIF2A is also shown through the connecting lines. They are linked by known interaction as experimentally determined (pink), as well association from text mining (yellow), co-

expression (black), gene neighborhood (green) and curated databases (blue). Figure generated with STRING (https://string-db.org).

A

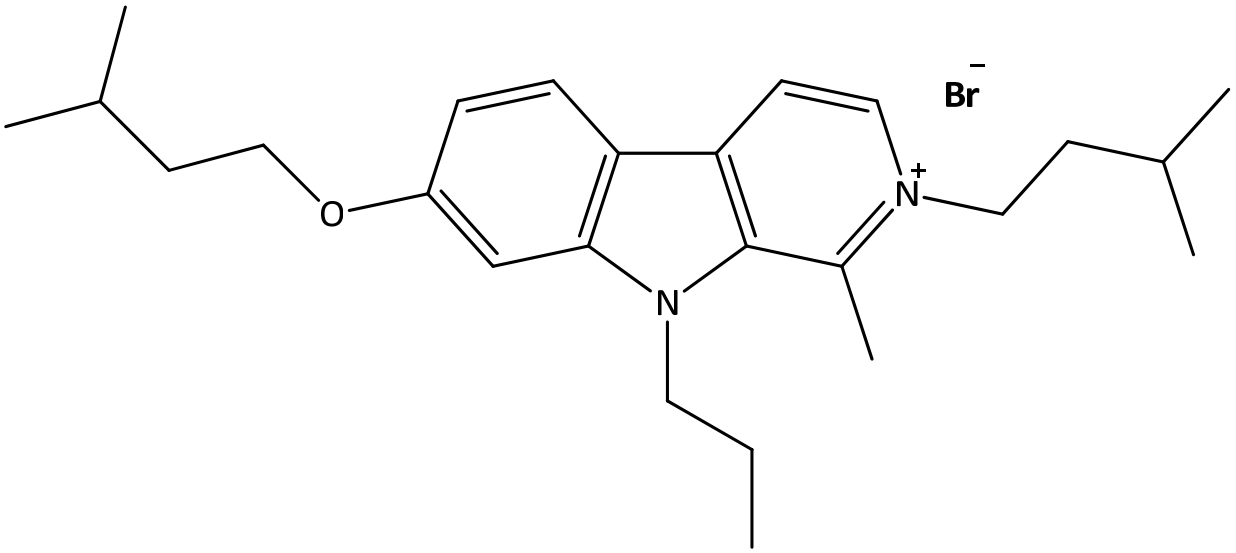
Br
O
N
N

B

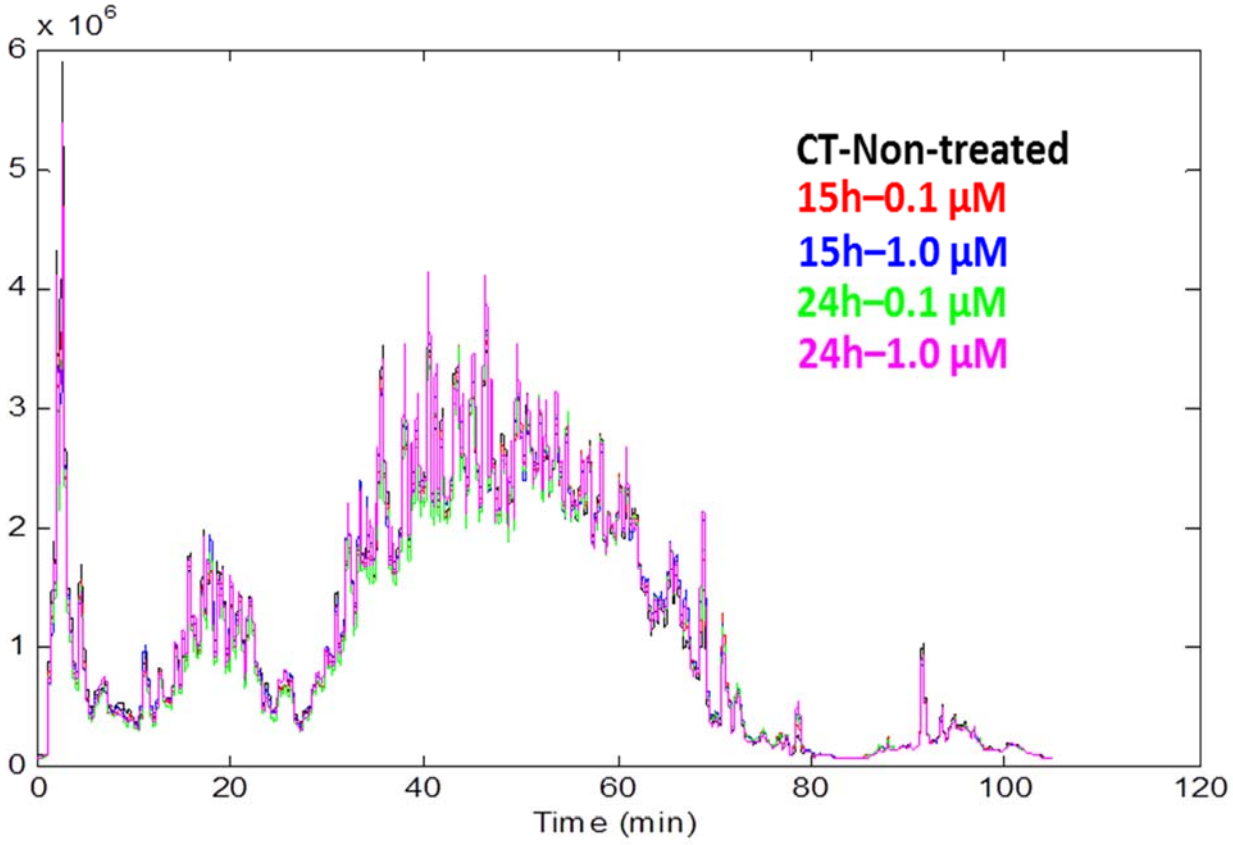
x 10^6
6
5
4
3
2
1
0
0
20
40
60
80
100
120
Time (min)
CT-Non-treated
15h–0.1 µM
15h–1.0 µM
24h–0.1 µM
24h–1.0 µM

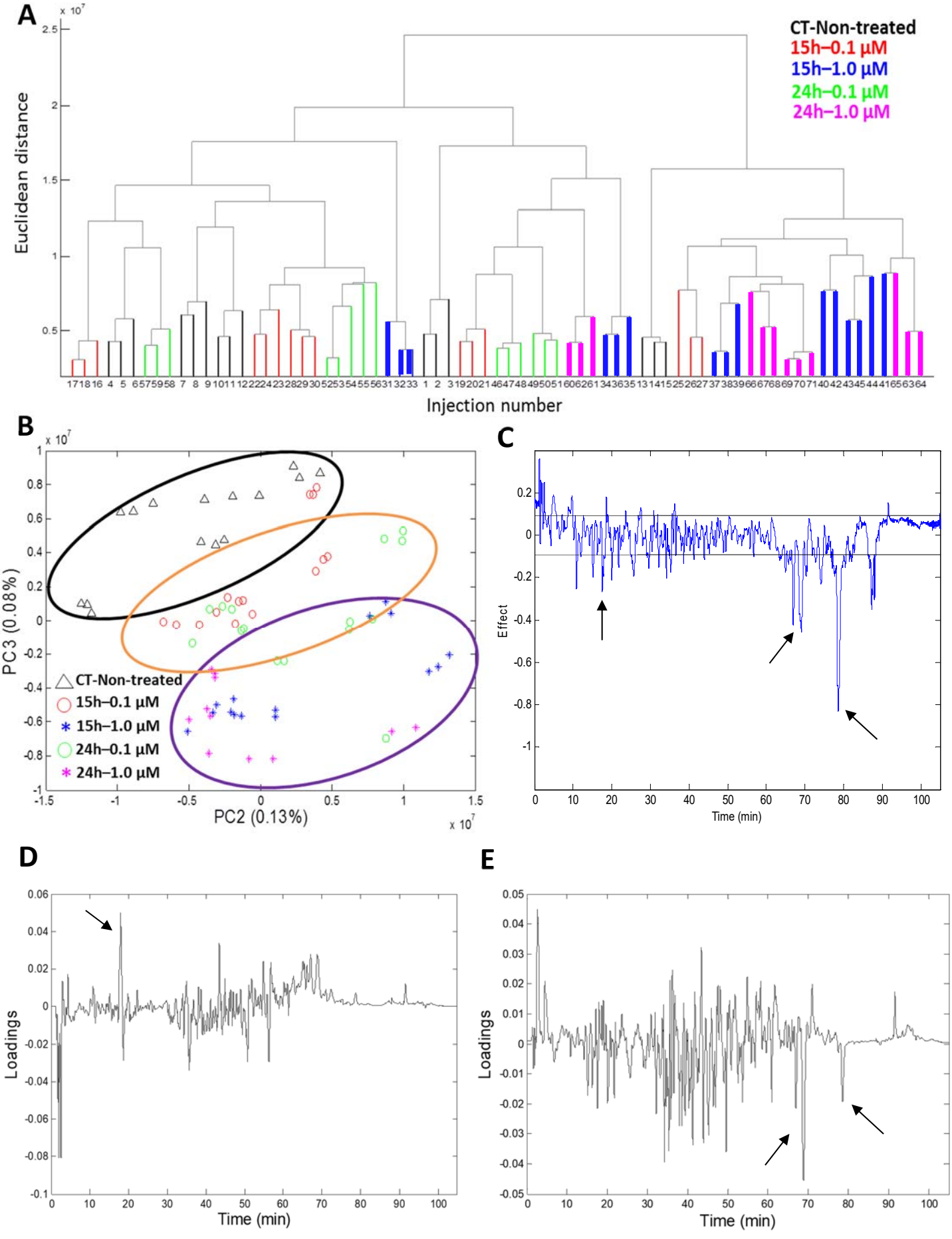
A
x 10^7
Euclidean distance
Injection number
CT-Non-treated
15h–0.1 µM
15h–1.0 µM
24h–0.1 µM
24h–1.0 µM
B
x 10^7
PC3 (0.08%)
PC2 (0.13%)
x 10^7
CT-Non-treated
15h–0.1 µM
15h–1.0 µM
24h–0.1 µM
24h–1.0 µM
C
Effect
Time (min)
D
Loadings
Time (min)
E
Loadings
Time (min)

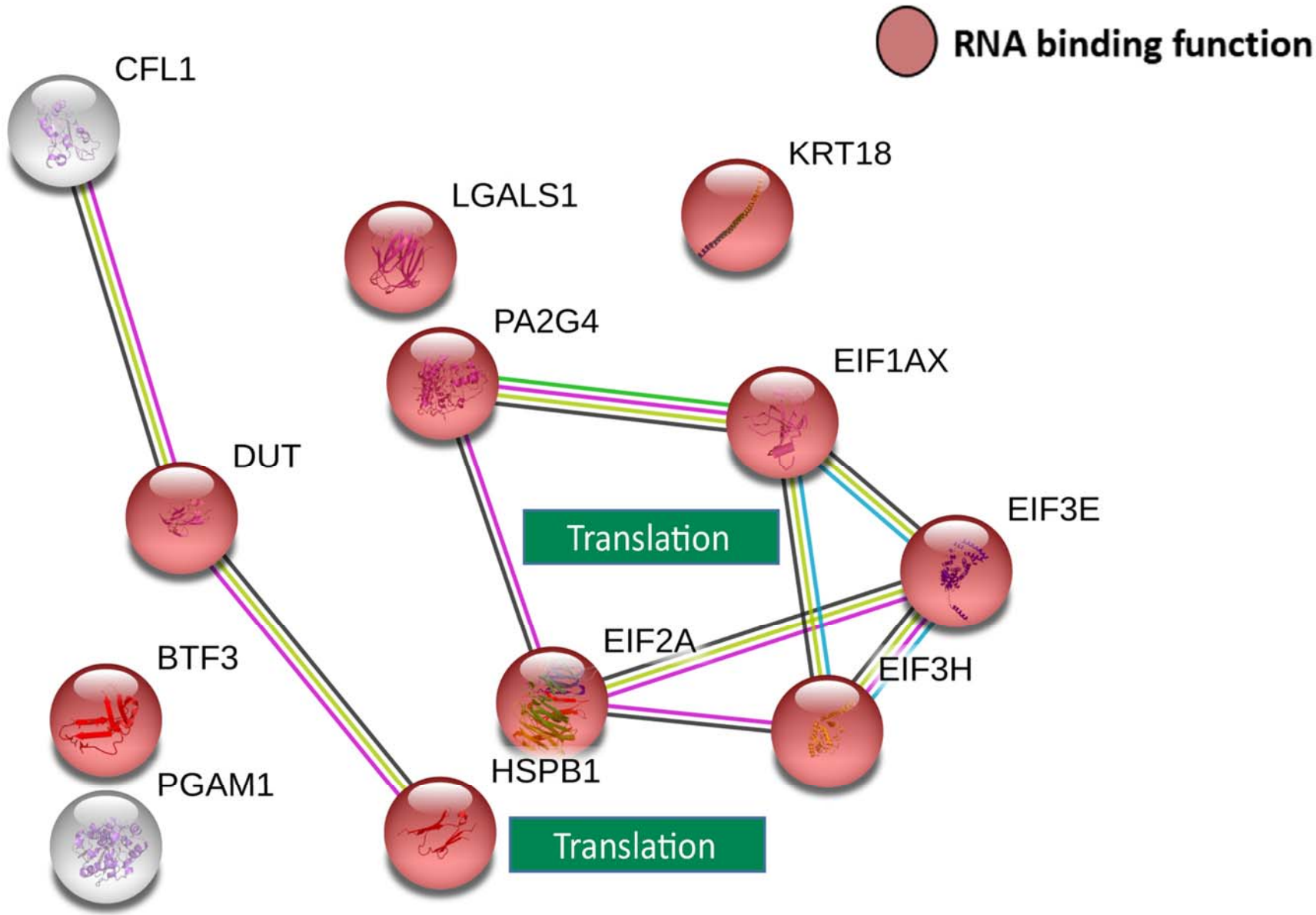
RNA binding function
CFL1
LGALS1
KRT18
PA2G4
EIF1AX
DUT
Translation
EIF3E
BTF3
EIF2A
EIF3H
PGAM1
HSPB1
Translation